Supporting Information

Pt-Graphene hybrid nanostructure as anode and cathode electrocatalyst in proton exchange membrane fuel cells

P. Divya and S. Ramaprabhu

Alternative Energy and Nanotechnology Laboratory (AENL), Nano Functional Materials Technology centre (NFMTC), Department of Physics, Indian Institute of Technology Madras, India. * Phone: +91-44-22574862; E-mail: ramp@iitm.ac.in

1. Structural analysis

Structural analysis of the samples (graphite, GO, L-ARGO, as grown MWNTs, air oxidized MWNTs, MWNTs, f-MWNTs) has been carried out by recording the powder XRD pattern. The peak centered at 2θ=26.5° (Fig. S1 (a)) corresponds to the (002) hexagonal planes of crystalline graphite. In Fig. S1 (b), shift of (002) peak to 2θ= 10° shows an increase in interlayer spacing. This confirms the successful oxidation of graphite by intercalation of oxygen containing functional groups. After reduction, the peak shifted back to 2θ = 26.5° with broadening indicates the removal of functional groups during reduction of GO and loss of long range order (Fig. S1(c)). In Fig. S1 (d-g) the diffraction peaks at 2θ=26.5° corresponds to (002) hexagonal graphitic plane. The other peaks denoted by '*' shows the presence of catalyst impurity ($MmNi_3$-H). The peaks for $MmNi_3$-H are not defined since after hydrogenation the material shows amorphization which results shift in peak position. The absence of $MmNi_3$-H peaks in MWNTs confirms removal of catalyst impurities by acid treatment.

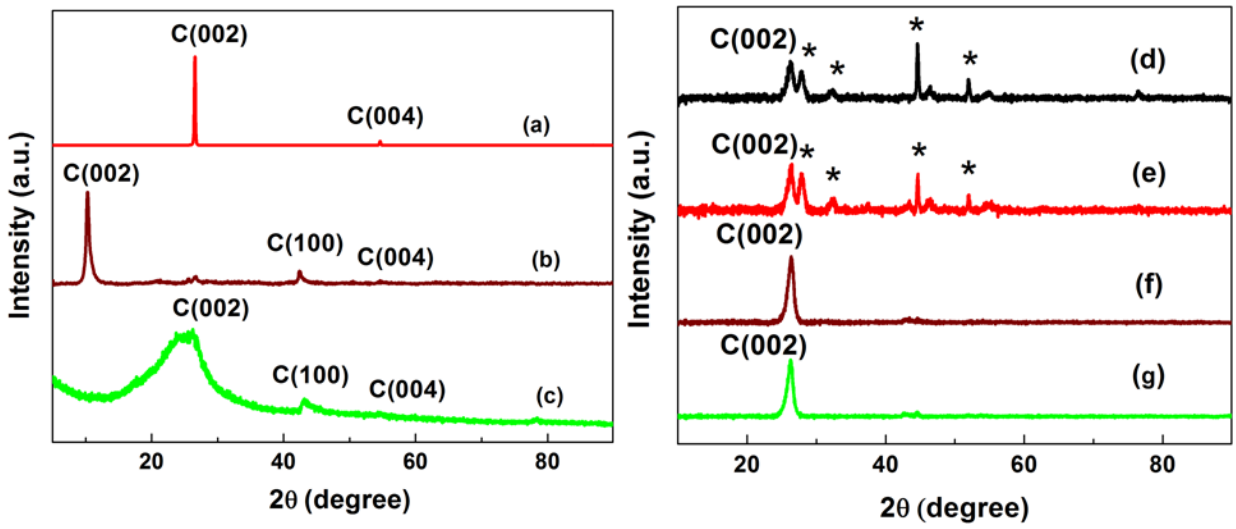

Fig. S1. XRD of (a) graphite, (b) GO, (c) L-ARGO, (d) as grown MWNTs, (e) air oxidized MWNTs, (f) MWNTs and (g) f-MWNTs.

An investigation of the functional groups present in graphite, GO and L-ARGO, MWNTs and f-MWNTs are done by FTIR analysis. Fig. S2 (a -c) show the FTIR spectra of Graphite, GO, Graphene. The graphite spectrum contains broad peak centered at 3454 cm^{-1} and 1624 cm^{-1} due to the vibrations of water molecules. The peaks at 2924 cm^{-1} and 2858 cm^{-1} represents symmetric and antisymmetric stretching vibrations of $–CH_2$ [1]. GO contains highly broadened and intense peaks at 3454 cm^{-1} and at l624 cm^{-1} indicates the stretching vibrations –OH represents that the GO samples contain large quantity of adsorbed water [2]. Intense peaks of C=O and C–O stretching vibrations of COOH groups at 1725 cm^{-1} and 1390 cm^{-1} can also be found [3]. After reduction the –OH functional groups are removed completely. The presence of peaks at 2924 cm^{-1} and 2858 cm^{-1} corresponding to the vibrations of $–CH_2$ [4]. The intensities of peaks at 1725cm^{-1}, 1370 cm^{-1} and 1390 cm^{-1} corresponding to C=O, C–O and –OH of COOH groups also reduced after reduction shows a partial removal of the these groups in the form of water vapour [5].

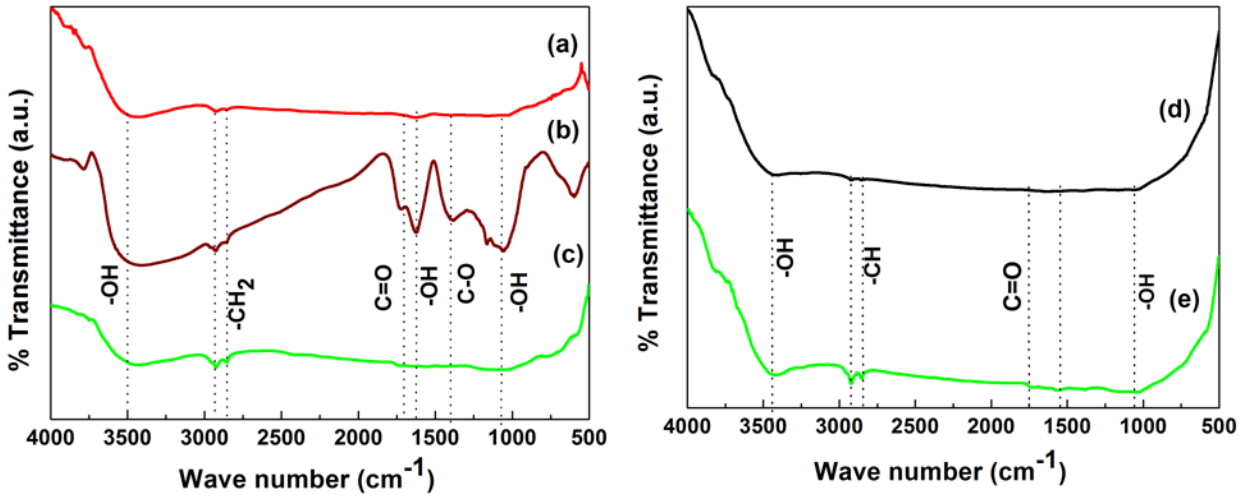

Fig. S2. FTIR spectrum of (a) graphite, (b) GO, (c) L-ARGO, (d) MWNTs and (e) f-MWNTs.

Functional groups on the surface of MWNTs by acid functionalization process act as anchoring sites for the attachment of metal nanoparticles. Fig. S2 (d & e) show the FTIR spectra of MWNTs and f-MWNTs. In f- MWNTs, a strong and broad peak can be seen around 3427 cm^{-1}, which corresponds to stretching mode of OH functional groups[6, 7] and bands around 2922 cm^{-1} and 2874 cm^{-1} are attributed to the asymmetric and symmetric stretching of C-H bond. The peak at 1634 cm^{-1} is due to the C=C stretching mode and the peak at 1384 cm^{-1} is due C-O stretching vibrations of COOH groups[8, 9].

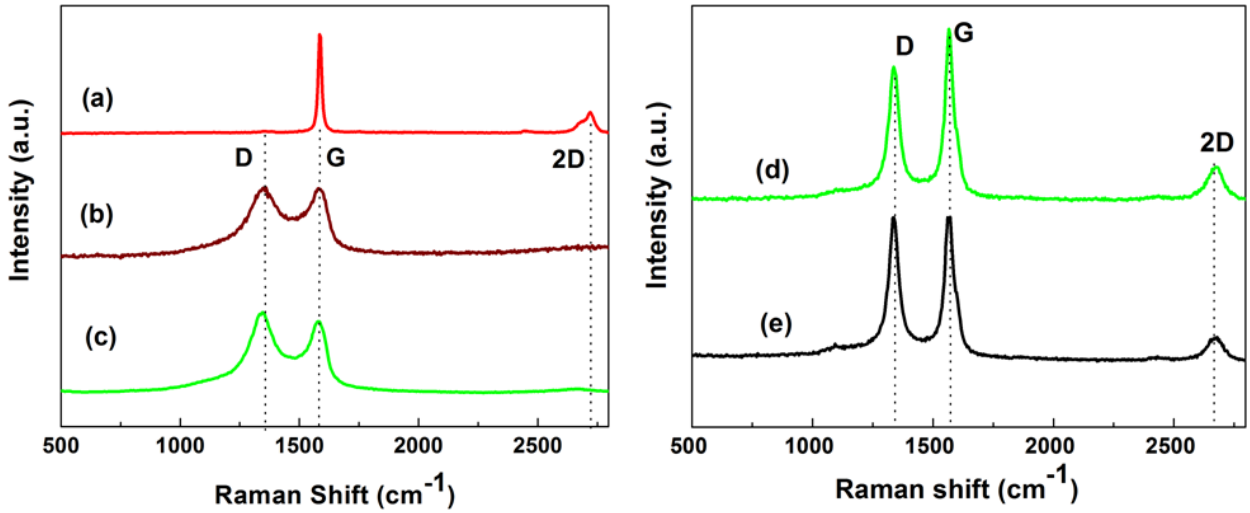

Fig. S3. Raman spectra of (a) graphite, (b) GO and (c) L-ARGO. (d) MWNTs and (e) f-MWNTs.

Raman spectroscopy is a tool which is used to identify carbonaceous samples from their vibrational spectra. Fig. S3 (a) – (c) shows the Raman spectra of graphite, GO, L-ARGO. The absence of the D- band peak in graphite indicates which is defect free. The presence of peak at 2717 cm^{-1} is the overtone of the D band called 2D band. G band, corresponding to the E_{2g} mode of sp^2 carbon atoms at 1582 cm^{-1} [10]. The G band of GO is located at 1596 cm^{-1}, while that of L-ARGO is shifted back to 1584 cm^{-1} due to the reduction of GO. The chemical treatments followed to obtain GO and its reduction to get L-ARGO induce defects in the graphitic structure. The ratio between the intensities of the D and G bands is used to identify the presence of defects in the samples. The ratio of the intensities of the D and G bands, I_D/I_G, is calculated to measure the degree of defects [11]. Fig. S3 (d & e) show the Raman spectra of purified MWNTs, f-MWNTs. the peak at 1576 cm^{-1} (G-band) is due to the Raman-active E_{2g} mode analogous to that of graphite [12], while the peak at 1348 cm^{-1} is D band , which is due to the defects or disorder present in MWNTs [13, 14]. The intensity of D-band is an indication of degree of disorder present in the nanotube. In f-MWNTs, the intensity of the D-band is higher since the functionalization adds carboxyl and hydroxyl functional groups on MWNTs which acts as anchoring sites for metal nanoparticles decoration. Table S1 shows the I_D/I_G ratio.

Table S1.I_D/I_G calculated from Raman spectra.

sample	I_D/I_G
MWNTs	0.95194
f-MWNTs	0.9788
Graphite	0.5923
GO	0.9975
L-ARGO	1.0458

2. FESEM and TEM images

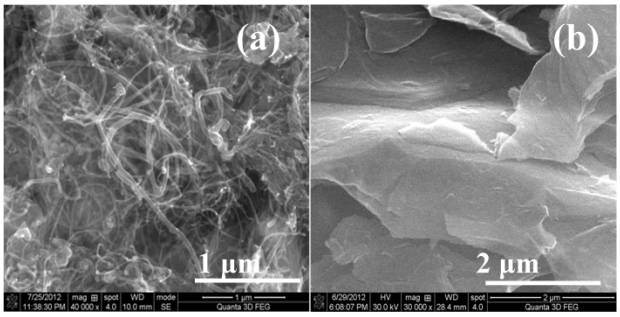

Fig. S4. FESEM images of (a) as grown MWNTs, (b) Graphite

3. Thermogravimetric analysis (TGA)

Fig. S5 shows the thermogravimetric analysis of Pt/L-ARGO and Pt/f-MWNTs in air atmosphere within a temperature range of room temperature to 1200 °C. TGA was carried out using a SDT Q600, TA instruments. The weight loss below 200 °C is observed due to the adsorbed water content in the sample. The weight percent shown after 700 °C is corresponding to loading level of platinum in the sample. The loading of platinum remaining in Pt/L-ARGO and Pt/f-MWNTs is 34 wt% and 30 wt% respectively.

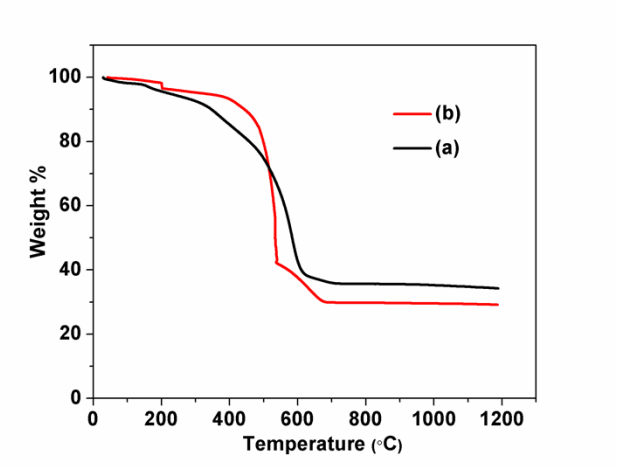

Fig. S5. TGA curve of (a) Pt/L-ARGO and (b) Pt/f-MWNTs

4. Polarization Curves

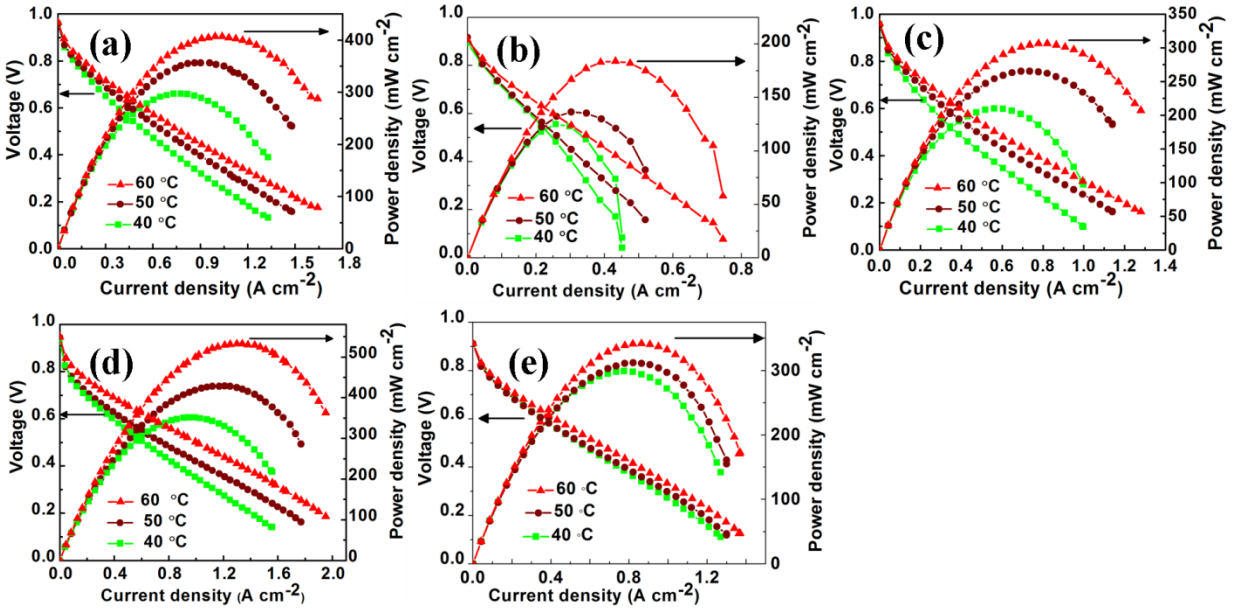

Fig. S6. Polarization curves recorded at 40 °C, 50 °C and 60 °C with one atmospheric back pressure for (a) MEA-1, (b) MEA-2, (c) MEA-3, (d) MEA-4 and (e) MEA-5

REFERENCES

1. G. I. Titelman, V. Gelman, S. Bron, R. L. Khalfin, Y. Cohen and H. Bianco-Peled, *Carbon*, 2005, **43**, 641-649.
2. X. Sun, Z. Liu, K. Welsher, J. Robinson, A. Goodwin, S. Zaric and H. Dai, *Nano Res.*, 2008, **1**, 203-212.
3. H.-K. Jeong, L. Colakerol, M. H. Jin, P.-A. Glans, K. E. Smith and Y. H. Lee, *Chemical Physics Letters*, 2008, **460**, 499-502.
4. G. Wang, B. Wang, J. Park, J. Yang, X. Shen and J. Yao, *Carbon*, 2009, **47**, 68-72.
5. W. Gao, L. B. Alemany, L. Ci and P. M. Ajayan, *Nat Chem*, 2009, **1**, 403-408.
6. W. Qian, T. Liu, F. Wei, Z. Wang, G. Luo, H. Yu and Z. Li, *Carbon*, 2003, **41**, 2613-2617.
7. N. I. Kovtyukhova, T. E. Mallouk, L. Pan and E. C. Dickey, *Journal of the American Chemical Society*, 2003, **125**, 9761-9769.
8. N. B. Colthup, L. H. Daly and Wiberlay, *Introduction to Infrared and Raman Spectroscopy*, Acadamic Press: Boston, 1990.
9. U. J. Kim, C. A. Furtado, X. Liu, G. Chen and P. C. Eklund, *Journal of the American Chemical Society*, 2005, **127**, 15437-15445.
10. S. Reich and C. Thomsen, *Philos. Trans. R. Soc. London, Ser. A*, 2004, **362**, 2271-2288.
11. C. C. Chuang, J. H. Huang, W. J. Chen, C. C. Lee and Y. Y. Chang, *Diamond and Related Materials*, 2004, **13**, 1012-1016.
12. A. C. Ferrari, *Solid State Communications*, 2007, **143**, 47-57.
13. M. S. Dresselhaus, A. Jorio, M. Hofmann, G. Dresselhaus and R. Saito, *Nano Letters*, 2010, **10**, 751-758.

14. A. C. Ferrari and J. Robertson, *Physical Review B*, 2000, **61**, 14095-14107.